Journal of Theoretical and Applied Physics (JTAP), Special Issue: AICIS'23-Article 07

Proceeding of the 3rd Annual International Conference on Information and Sciences 2023, University of Fallujah, Iraq

https://dx.doi.org/10.57647/j.jtap.2024.si-AICIS23.07

Influence of heat treatment on the efficiency of WO_3: Au NPs optoelectronic device prepared by spray pyrolysis technique

Mohammed Hamid Mustafa*, Aliyah A. Shihab

Department of Physics, College of Education for Pure Science Ibn Al-Haitham, University of Baghdad, Baghdad, Iraq.

***Corresponding author:** mohammed.h.m@ihcoedu.uobaghdad.edu.iq

Original Research

Published online: 15 June 2024

Abstract:

By using pyrolysis spray technique, tungsten dioxide films doped with gold nanoparticles were successfully deposited on glass and silicon substrates at 320 °C. Au-WO_3 films were annealed for one hour at 673 (K) and 873 (K). A number of physical characteristics of the prepared and annealed films have been examined using atomic force microscopy, UV-visible spectroscopy, X-ray diffraction and other techniques. It was discovered that the indirect energy gap in the UV-visible spectrum of as-prepared and annealed thin films decrease after annealing from 2.86 eV to 2.42 eV, and according to the structure properties, the prepared and annealed thin films had an amorphous structure at substrate temperature 320 °C, but they had a polycrystalline structure at annealing temperature. The samples' cubic structures for gold nanoparticles and monoclinic structures for tungsten trioxide were also revealed. The thin layer of all sample can be seen to have a nanostructure thanks to atomic force microscopy. All prepared films, whether doped with gold, or those that have been annealed at 673,873 (K), are shown by Hall effect measurements to have a negative Hall coefficient. This indicates that prepared films are of n-type, and have highest conductivity and mobility of carriers, respectively 10.52×10^{-5} $\Omega.cm^{-1}$ and 476.45 cm^2/V.S, and that the highest efficiency of the WO_3: Au/Si (1.804%) was attained when measurements current-volt under illumination.

Keywords: Structural; Optical properties; Plasmon; Efficiency; WO_3: GNPs thin films

1. Introduction

Researchers have become more interested in metal oxides as potential options for a wide range of applications as a result of the advancement of nanotechnology and synthetic techniques. As a working electrode in gas sensors, electrochromic windows, displays, anti-glare rearview mirrors, photocatalysis, tungsten oxide (WO_3) is a versatile n-type semiconductor [1–3]. WO_3 has a monoclinic crystal structure with a wide band gap (E_g) ranged about $2.5 - 3.2$ eV [4, 5]. This substance stands out for a variety of reasons, such as its low cost, chemical stability, non-toxicity, and mechanical capabilities; it is also regarded as a catalyst for semiconductors [6, 7]. Because of its contemporary magnetic, chemical, and physical properties, Au nanoparticles stand out among noble metals in many ways [8, 9]. Pure WO_3 films can be made more elaborate by mixing it with minute amounts of GNPs [10]. Due to their size-dependent effects, such as strong optical absorbance brought on by surface plasmon resonance, gold nanostructures are often used [11, 12]. Electron beam deposition or evaporation, thermal evaporation, laser deposition, radio-frequency sputtering, anodic oxidation, sol-gel, hydrothermal, and spray pyrolysis, and other processes have all been utilized to produce WO_3 thin films [13, 14]. In this research the main objective of preparing this work is to study the effect annealing on the efficiency photovoltaic of WO_3: Au/Si at 873 (K) prepared by chemical spray pyrolysis method.

2. Experimental details

The spray pyrolysis method is used to prepare tungsten trioxide films doped with gold nanoparticles with a thickness of 250 nm in this work. Spraying the solution on a hot glass and silicon wafer (p-type) deposited thin films and fabricated Al/WO_3: Au/Si/Al device. The chemical reaction of

the prepared solution on the hot substrate will result in the formation of the film that have been primed and cleaned at a temperature of about 320 °C. Set the distance between the nozzle and the substrates to about 25 cm.
Prepare the film deposition solution by using tungstic acid H_2WO_4 as the tungsten source material. Distilled water is the most commonly used solvent, but H_2WO_4 does not dissolve in water. So, for un-doped WO_3, a 0.06 M concentration solution is prepared by dissolving H_2WO_4 in distilled water with a small amount of ammonia solution [15]. For 30 minutes, the solution is mixed through a magnetic starrier. The source material of Au doped WO_3 has been accepted as chloroauric acid ($HAuCl_4$) 6 mM from $HAuCl_4$ mixed with WO_3 solution for preparing Au doped WO_3 thin films according to the following Equation (1) [16]:

$$W_t = M.Mwt.V \tag{1}$$

where W_t: weight of the material, M: molecular concentration, Mwt: molecular weight, V: volume.
Many tests, including XRD, UV-Vis, AFM, Hall effect and current–voltage (under illumination) were used to examine the produced samples.

3. Results and discussion

3.1 Structural analysis

3.1.1 XRS analysis

Fig. 1 displays the XRD patterns of the deposited WO_3: Au NPs thin films and those annealed at different temperatures (673, 873 K). The thin films of WO_3: Au NPs have an amorphous structure at Ts = 320 °C, which agrees with Naseri [17]. The peak at 2θ = 38.213° represents the formation of the cubic phase of gold at the (111) direction, these results agree with Ibrahim [16], and with the numbered card CAS (7440-57-5). The crystalline size of the tungsten trioxide films doped with gold nanoparticles is 10.05 nm. The Scherer equation was used to calculate the average crystal size [18]:

$$c.s = \frac{0.94\lambda}{\beta \cos\theta} \tag{2}$$

where β is the full width at half maximum (FWHM), λ is the wavelength which equals 0.154 nm of XRD photons, and θ is the Brage diffraction angle in degrees.
The following equation can be used to determine the micro strain (ε) for manufactured thin films [19]:

$$\varepsilon = \frac{\beta \cos\theta}{4} \tag{3}$$

The formula below can be used to calculate the dislocations density δ, which is defined as the length of dislocation lines per unit volume of the crystal [20].

$$\delta = \frac{1}{(c.s)^2} \tag{4}$$

After an hour of annealing in the presence of air at various temperatures (673, 873 K), samples of WO_3 doped with Au NPs developed the crystalline structures depicted in Fig. 1 and Table 1. Reflections at the angles specified in Table 1 were determined to be reflections of the monoclinic WO_3 phase [4, 17, 21], in accordance with the CAS number (1314-35-8).

3.1.2 AFM analysis

Fig. 2 displays a two-dimensional images of tungsten trioxide films doped with gold nanoparticles WO_3: Au, whether annealed at different annealing temperatures or un annealed by using an atomic force microscope (AFM). The surface of WO_3: Au sample is tightly packed and has a completely organized granular structure. As shown in Table 2, the grain size of the doped films increased with increasing annealing temperatures, this increase is expected because the crystalline size of these films increases with increasing annealing temperature, which can cause recrystallization in the grains [22]. This result is similar to the results obtained by Ibrahim and Hasan [16, 23].

3.2 Optical properties

The produced thin films optical transmittance spectra were captured in the (350–1000 nm) wavelength range. On the surface plasmon resonance and energy band gap (E_g), the impact of annealing at different temperatures are investigated. In general, the transmittance of tungsten oxide coatings reduces when gold is added. It might be due to greater absorption, which could be connected to the distortion brought on by the Au ions in WO_3.
The optical transmittance and absorbance spectra of prepared and annealed thin films are displayed in Fig. 3. Table 3 displays a collection of data from several investigations on WO_3: Au nanocomposites with full width at half maximum (FWHM) and the LSPR peak location (λ_{SPR}). The average transmittance of WO_3: Au film is 67%. These films show an ordered decrease in transmittance with the addition of gold and annealing the doped sample. The transmittance spectra of the gold-incorporated film exhibit a dip at about 595 nm, which may be the result of absorption brought on by the gold nanoparticles' surface plasmon resonance (SPR). The present of gold nanoparticles in tungsten trioxide films is mostly responsible for the LSPR absorption band's intensity rise with temperature [24, 25].
As the annealing temperature changes, the LSPR peak po-

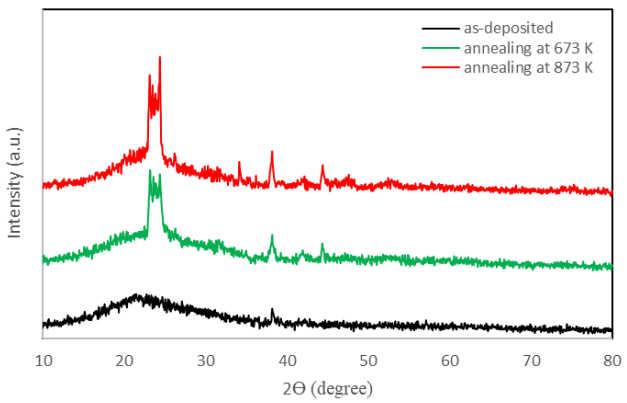

Figure 1. XRD pattern for WO_3: Au at various annealing temperature.

sition also shifts (Fig. 3), with orange moving away from SPRAD at 595 nm and yellow moving back to LSPR 873 (K) at 575 nm, this behavior is similar to the behavior of tungsten oxide films after adding gold in [26]. By extrapolating the straight line section of the $(\alpha h\nu)^{1/2}$ versus $(h\nu)$, the band gap values of WO_3: Au NPs thin films (as-deposited and at various annealing temperatures) may be calculated (see Fig. 4). From Fig. 4 demonstrates that (E_g) can be seen to be somewhat decreasing for thin films at annealing temperature Ta = 873 (K), because WO_3 experiences oxygen deficit at higher annealing temperatures [27]. These findings concur with those of H. Simchi [4], which may be a result of the interaction between the dopant and annealing temperature.

Because it was discovered that the dependency of absorption coefficient (α) on the photon energy $(h\nu)$ obeyed the following relationship [28, 29], the type of transition was indirectly permitted:

$$\alpha h\nu = K(h\nu - E_g)^r \tag{5}$$

$$\alpha = 2.303\frac{A}{t} \tag{6}$$

where r is a characteristic number of the transition process, with $r = 2$ for direct allowed transitions, $r = 2/3$ for direct forbidden transitions, $r = 1/2$ for indirect allowed transitions, and $r = 1/3$ for indirect forbidden transitions; K is a parameter that depends on the electron-hole mobility; $h\nu$ is the photon energy; (A) is absorbance and (t) is thickness of films. The presence of GNPs makes the values of absorption coefficient (α) in this study's doped tungsten trioxide films appear high. They reach their highest value (7.54 cm^{-1}) at $\lambda_{SPR} = 575$ (nm) when doped films are annealed at (873 K).

3.3 Electrical properties

Thin films of WO_3 that have been doped with gold nanoparticles, and WO_3: Au which are annealed at various temperatures, shows variations in carrier concentration (n_H) and Hall mobility (μ_H), as seen in Fig. 5. Hall measurements re-

Table 1. X-ray diffraction parameters for WO_3: Au NPs thin films at (673, 873 K).

Ta (K)	2θ (deg.) Exp.	d (A°) ASTM	d (A°) Exp.	Planes (hkl)	Phase	FWHM (deg.)	C.S (nm)	$\delta \times 10^{15}$ (lines/m^2)	$\varepsilon \times 10^{-3}$
673	23.202	3.8440	3.8428	(002)	Mon. WO_3	0.4674	18.1206	3.04548	1.9972
	23.619	3.7690	3.7673	(020)	Mon. WO_3	0.5812	14.5837	4.70184	2.4816
	24.419	3.6480	3.6469	(200)	Mon. WO_3	0.5134	16.5344	3.65784	2.1888
	38.208	2.3550	2.3547	(111)	Cub. Au	0.8243	10.6557	8.8072	3.3963
	44.337	2.0390	2.0383	(200)	Cub. Au	0.9887	9.06666	12.1648	3.9916
873	23.142	3.8440	3.8437	(002)	Mon. WO_3	0.4012	21.1083	2.2444	1.7145
	23.513	3.7690	3.7684	(020)	Mon. WO_3	0.4839	17.5126	3.2606	2.0665
	24.389	3.6480	3.6478	(200)	Mon. WO_3	0.4311	19.6898	2.5794	1.8380
	34.162	2.6230	2.6227	(202)	Mon. WO_3	0.5071	17.1202	3.4118	2.1139
	38.187	2.3550	2.3548	(111)	Cub. Au	0.6381	13.7642	5.2784	2.6293
	44.389	2.0390	2.0393	(200)	Cub. Au	0.5732	15.6418	4.0872	2.3137

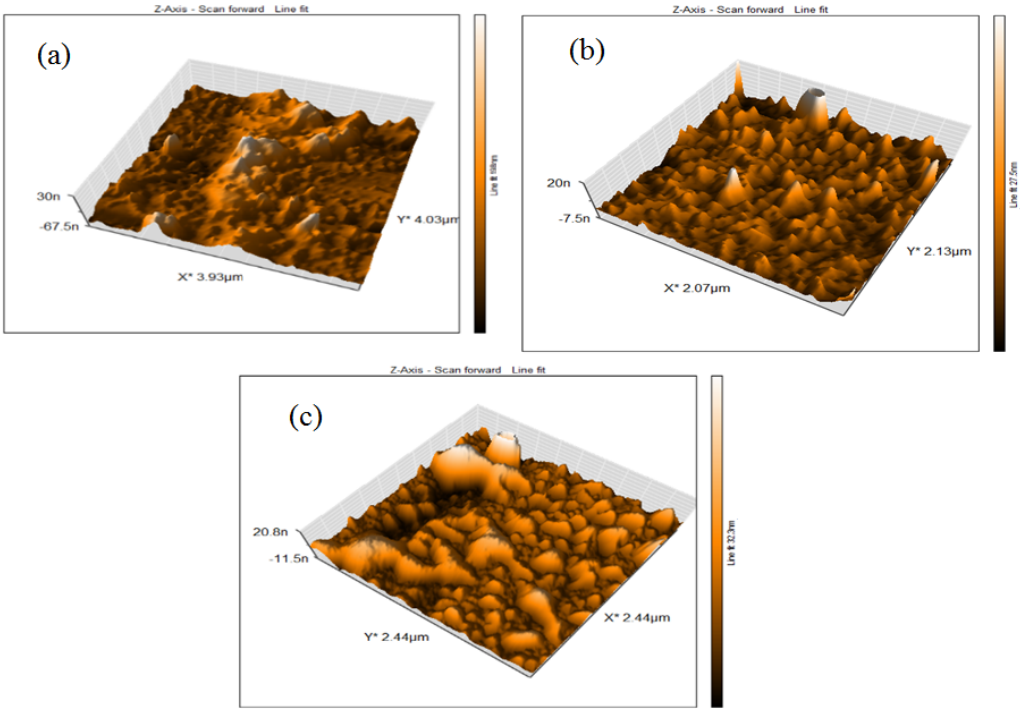

Figure 2. AFM images of WO_3: Au thin films. (a) as-deposited, (b) annealed at 673 (K) and (c) annealed at 873 (K).

veal that all of these films exhibit a negative Hall coefficient (n-type charge carriers); this result is consistent with [30]. Table 4 demonstrates that the types of charge carriers are unaffected by the annealing procedures, and that the conductivity of the doped film increased after annealing. This is caused by the fact that it is a semiconductor and has a negative heat coefficient. We see from Fig. 5 and Table 4 that the concentration of the carrier's decreases, while the mobility of the carriers increases by annealing tungsten trioxide films doped with gold nanoparticles due to the improvement in crystal structure and decrease in grain boundaries and crystalline defects of the films after annealing.

With a voltage range of 0 to 0.6 (Volt), Fig. 6 depicts the current and voltage densities of an Al/WO_3: Au/Si/Al solar cell under illumination.

Table 5 shows that heat treatment of tungsten trioxide films doped with gold nanoparticles leads to an increase in the photoelectric efficiency of Al/WO_3: Au/Si/Al from (1.548%) to (1.804%), when the annealing temperature of WO_3: Au films is raised to a temperature of (873 K) for one hour. Because the surface area of the sample grows as a result of the addition of gold particles, the crystal structure also improves as a result of the decrease in oxygen content in the annealed sample [27]. Since sunlight helps enhance the production efficiency of solar cells, it may be beneficial to encourage faster electron transit while reducing the possibility of electron-hole pair recombination.

4. Conclusion

At 320 °C, tungsten trioxide films doped with gold nanoparticles at molar concentrations (0.06, 0.006 M) of (WO_3, Au) were efficiently produced on glass and silicon substrates. The doped films formed at Ts = 320 °C show an amorphous structure in the XRD pattern, but after WO_3: Au annealing at 873 K, they were found to have a polycrystalline structure. The phenomenon of surface plasmon resonance appeared in tungsten trioxide films doped with gold nanoparticles. It was found that raising the annealing temperature led to a reduction in the energy gap and particle size, while the conductivity and mobility of the carriers of the prepared and annealed films increased. With the same preparation conditions, in addition to obtaining the highest photoelectric efficiency at different annealing temperatures.

Table 2. Grain size (nm), roughness average (nm) and root mean square (nm).

Samples	Grain size (nm)	Roughness average (nm)	Root mean square (nm)
As-deposited	47.85	11.71	16.39
Annealed at 673 K	59.01	40.58	51.59
Annealed at 873 K	79.90	66.10	94.73

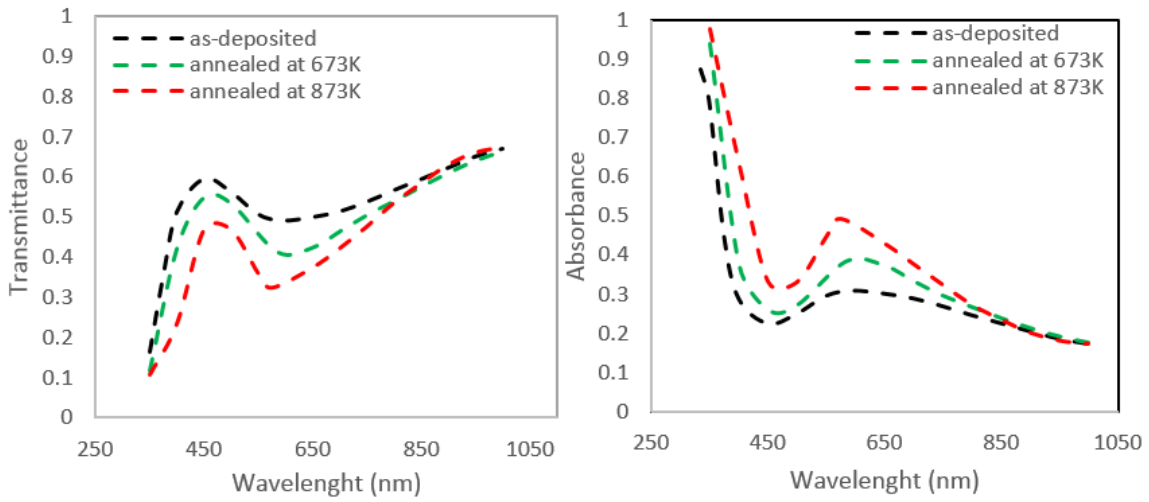

Figure 3. Transmittance and absorbance spectrum as function of wavelength for WO_3: Au thin films at various annealing temperatures.

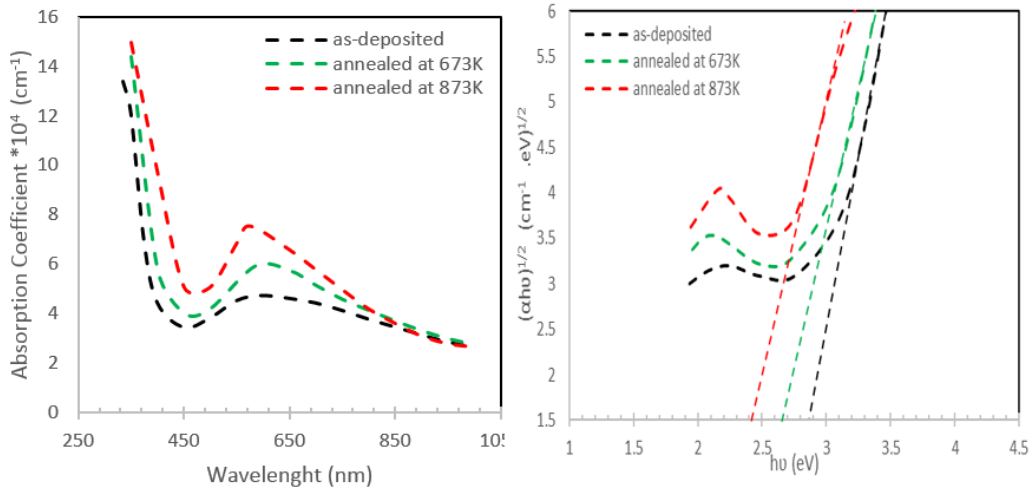

Figure 4. Absorption coefficient and Energy gap for WO_3: Au thin films at different annealing temperature.

Table 3. Energy gap (E_g), full-width at half maximum (FWHM) and peak position (λ_{SPR}) of the prepared and annealed samples.

Annealing temperature (K)	E_g (eV)	FWHM (nm)	λ_{SPR} (nm)
As-deposited	2.86	327	595
673	2.67	255	285
873	2.42	200	575

Table 4. Electrical characteristics of WO_3: Au thin films at various temperatures.

Annealing temperature (K)	$R_H \times 10^6$ (cm^3/C)	$n_H \times 10^{12}$ (cm^{-3})	μ_H (cm^2/V.S)	$\sigma \times 10^{-5}$ $(\Omega.cm)^{-1}$
As-deposited	-3.30	1.90	224.00	6.79
673	-3.81	1.64	300.92	7.89
873	-4.53	1.38	476.45	10.52

Table 5. Current–Voltage characteristics of WO_3: Au/Si thin films at different annealing temperatures.

Annealing temperature (K)	J_{SC} (mA/cm^2)	V_{OC} (volt)	J_m (mA/cm^2)	V_m (Volt)	η %
As-deposited	4.7	0.56	3.6	0.43	1.548
673	5.22	0.565	3.9	0.434	1.6926
873	5.67	0.58	4.1	0.44	1.804

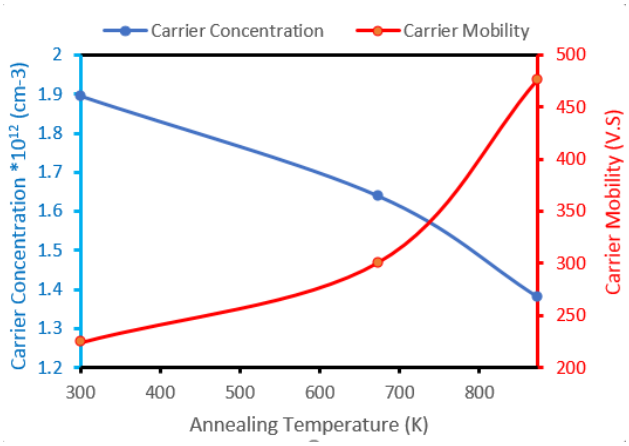

Figure 5. Carrier concentration and mobility as a function of annealing temperature.

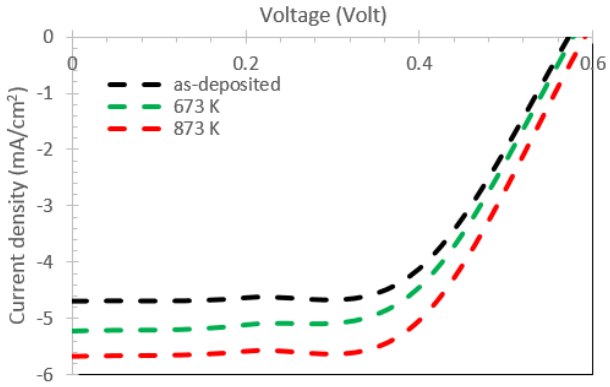

Figure 6. J-V characteristic for WO_3: Au/Si heterojunction at different annealing temperature.

Ethical approval
This manuscript does not report on or involve the use of any animal or human data or tissue. So the ethical approval is not applicable.

Authors Contributions
All the authors have participated sufficiently in the intellectual content, conception and design of this work or the analysis and interpretation of the data (when applicable), as well as the writing of the manuscript.

Availability of data and materials
The datasets generated and analyzed during the current study are available from the corresponding author upon reasonable request.

Conflict of Interests
The author declare that they have no known competing financial interests or personal relationships that could have appeared to influence the work reported in this paper.

References

[1] M. Deepa, D. P. Singh, S. M. Shivaprasad, and S. A. Agnihotry. "A comparison of electrochromic properties of sol–gel derived amorphous and nanocrystalline tungsten oxide films.". *Curr. Appl. Phys.*, **7**:220–229, 2007.

[2] I. H. Khudayer, B. H. H. Ali, M. H. Mustafa, and A. J. Ibrahim. "Investigation of the structural, optical and electrical properties of $AgInSe_2$ thin films.". *Ibn AL-Haitham J. Pure Appl. Sci.*, **31**:37–49, 2018.

[3] M. H. Mustafa. "Fabrication and characterization CdO: In/Si photovoltaic solar cell prepard by thermal evaporation.". *Ibn AL-Haitham J. Pure Appl. Sci.*, **27**: 273–278, 2017.

[4] H. Simchi, B. E. McCandless, T. Meng, and W. N. Shafarman. "Structural, optical, and surface properties

of WO_3 thin films for solar cells.". *J. Alloys Compd.*, **617**:609–615, 2014.

[5] J. O. R. de León, D. R. Acosta, U. Pal, and L. Castaneda. "Improving electrochromic behavior of spray pyrolised WO_3 thin solid films by Mo doping.". *Electrochimica Acta.*, **56**:2599–2605, 2011.

[6] K. J. Patel, C. J. Panchal, V. A. Kheraj, and M. S. Desai. "Growth, structural, electrical and optical properties of the thermally evaporated tungsten trioxide (WO_3) thin films.". *Mater. Chem. Phys.*, **114**:475–478, 2009.

[7] S. K. Gullapalli, R. S. Vemuri, and C. V. Ramana. "Structural transformation induced changes in the optical properties of nanocrystalline tungsten oxide thin films.". *Appl. Phys. Lett.*, **96**, 2010.

[8] A. A. Shehab, S. A. Maki, and A. A. Salih. "The structural and surface morphology properties of aluminum doped CdO thin films prepared by vacuum thermal evaporation technique. ". *Ibn AL-Haitham J. Pure Appl. Sci.*, **27**:158–169, 2017.

[9] H. Mumtaz and I. H. Khudayer. "Influence annealing on the physical properties of silver selenide thin film at different temperatures by thermal evaporation. ". *Ibn AL-Haitham J. Pure Appl. Sci.*, **36**:147–155, 2023.

[10] G. H. Mohammed. "The effect of Au nanoparticles on the structural and optical properties of (NiO: WO_3) thin films prepared by PLD technique.". *Iraqi J. Sci.*, : 2502–2513, 2022.

[11] J. Nagai, G. D. McMeeking, and Y. Saitoh. "Durability of electrochromic glazing. ". *Sol. Energy Mater. Sol. Cells.*, **56**:309–319, 1999.

[12] T. He, Y. Ma, Y. Cao, W. Yang, and J. Yao. "Enhanced electrochromism of WO_3 thin film by gold nanoparticles. ". *J. Electroanal. Chem.*, **514**:129–132, 2001.

[13] F. A. Mohammed, E. T. Salim, A. I. Hassan, and M. H. Wahid. "Effect of precursor concentration on the structural, optical, and electrical properties of WO_3 thin films prepared by spray pyrolysis.". *J. Appl. Sci. Nanotechnol.*, **2**:91–105, 2022.

[14] H. M. Ali and M. H. Mustafa. "Optimization physical properties of CdTe/Si solar cell devices fabricated by vacuum evaporation.". *Chalcogenide Lett.*, **20**: 431–437, 2023.

[15] M. Arifuzzaman. "Investigation of silver doping on structural, optical and electrical properties of spray deposited tungsten trioxide thin films. ". , 2021.

[16] I.M. Ibrahim. "The effect of gold nanoparticles on WO_3 thin film.". *Iraqi J. Phys.*, **16**:11–28, 2018.

[17] N. Naseri, R. Azimirad, O. Akhavan, and A. Z. Moshfegh. "Improved electrochromical properties of sol–gel WO_3 thin films by doping gold nanocrystals.". *Thin Solid Films.*, **518**:2250–2257, 2010.

[18] B. D. Cullity. "Elements of X-ray diffraction. ". *Addison-Wesley Publishing*, , 1956.

[19] V. D. Karan, X. S. Shajan, and S. T. Karasan. "X-Ray line Broadening and Photo elector chemical Studies. ". *J. Mater. Sci.*, **46**:4034–4045, 2011.

[20] S. Chander, A. Purohit, C. Lal, and M. S. Dhaka. "Enhancement of optical and structural properties of vacuum evaporated CdTe thin films.". *Mater. Chem. Phys.*, **185**:202–209, 2017.

[21] M. Raja, J. Chandrasekaran, M. Balaji, and B. Janarthanan. "Impact of annealing treatment on structural and dc electrical properties of spin coated tungsten trioxide thin films for Si/WO_3/Ag junction diode.". *Mater. Sci. Semicond. Process.*, **56**:145–154, 2016.

[22] A. Z. Obaid, M. H. Mustafa, and H. K. Hassun. "Studying the effect of the annealing on Ag_2Se thin film. ". *AIP Conference Proceedings*, **2307**:020007, 2020.

[23] S. F. Hasan, A.-M. E. Al-Samarai, A. S. Obaid, and A. Ramizy. "Study the structure and optical properties of GNPs doped WO_3/PS by spray pyrolysis deposition (SPD).". *IOP Conf. Ser. Mater. Sci. Eng.*, :012011, 2021.

[24] C. Louis and O. Pluchery. "Gold nanoparticles for physics, chemistry and biology. ". *World Scientific*, , 2017. DOI: https://doi.org/10.1142/q0036 — August 2017.

[25] U. Kreibig and M. Vollmer. "Optical properties of metal clusters.". *Springer Science & Business Media*, , 2013.

[26] N. M. Figueiredo, F. Vaz, L. Cunha, and A. Cavaleiro. "Au-WO_3 nanocomposite coatings for localized surface plasmon resonance sensing.". *Materials*, **13**:246, 2020.

[27] M. H. Mustafa and A. A. Shihab. "Effect of ratio gold nanoparticles on the properties and efficiency photovoltaic of thin films of amorphous tungsten trioxide.". *Journal of Ovonic Research*, **19**:623–630, 2023.

[28] M. G. Hutchins, O. Abu-Alkhair, M. M. El-Nahass, and K. Abd El-Hady. "Structural and optical characterisation of thermally evaporated tungsten trioxide (WO_3) thin films. ". *Mater. Chem. Phys.*, **98**:401–405, 2006.

[29] M. Hamid, S. A. Fadaam, L. A. Mohammed, and B. H. Hussein. "Influence of addition (Mn) on enhance efficiency of ($CuInTe_2$) photovoltaic cell. ". *Eurasian Chem.-Technol. J.*, **21**:183–185, 2019.

[30] V. V. Ganbavle, G. L. Agawane, A. V. Moholkar, J. H. Kim, and K. Y. Rajpure. "Structural, optical, electrical, and dielectric properties of the spray-deposited WO_3 thin films. ". *J. Mater. Eng. Perform.*, **23**:1204–1213, 2014.